

A. Predicting the Onset of High-Speed GMA Weld Defects

by T. C. Nguyen, Conestoga College; D. C. Weckman, D. Johnson, University of Waterloo

Introduction

The geometric defects such as undercut or humped weld beads frequently prevent achievement of higher welding speeds and increased productivity when using various fusion welding processes. The occurrence of these high-speed weld defects can be documented on a process map of welding speed versus welding power while keeping other influential process parameters constant. However, small changes to any of the other process parameters in these multivariate welding processes will invalidate the process map. Thus, more experimental work is needed to create a new process map which is valid only for this new combination of process parameters. In the present study, dimensional analysis is utilized to reduce the dimensionality of the multivariate gas metal arc welding (GMAW) process thereby allowing the formulation of a dimensionless process map that can be used to predict the onset of high-speed weld defects as a function of all influential process parameters.

Procedure

Using a robotic welding system, a process map was generated for GMA steel welds produced using 0.9 mm (0.035") diameter ER70S6 wire, three different shielding gases; Argon, Mig Mix Gold™ or MMG™ (Ar-8%CO₂) and TIME™ gases (Ar-26.5%He-8%CO₂-0.5%O₂), between 5 kW and 12 kW welding power and a wide range of welding speeds. For each combination of process parameters, the maximum or limiting welding speed that produced a good weld bead was determined. Dimensional analysis using Buckingham's theorem was utilized to identify a number of dimensionless groups formulated from various combinations of the influential GMAW process parameters and the material properties. The process map was then re-plotted using these dimensionless groups to show the onset of high-speed weld defects as a function of all influential process parameters.

Results and Discussion

Dimensional plots of the limiting welding speed versus welding power clearly exhibited regions of process parameters that produced good and defective weld beads (see Figure 1a). In addition, the limiting welding speed data was stratified according to the shielding gas used. At lower welding powers, when spray transfer mode occurred, the limiting welding speed of welds made using MMG™ and TIME™ shielding gases had 400-600% higher limiting welding speeds than those obtained with Argon shielding gas. However, the observed difference decreased with the increased welding power. When the welding power was increased above 9 kW, the filler metal transfer mode switched from spray to rotational transfer and the limiting welding speed became independent of the welding power.

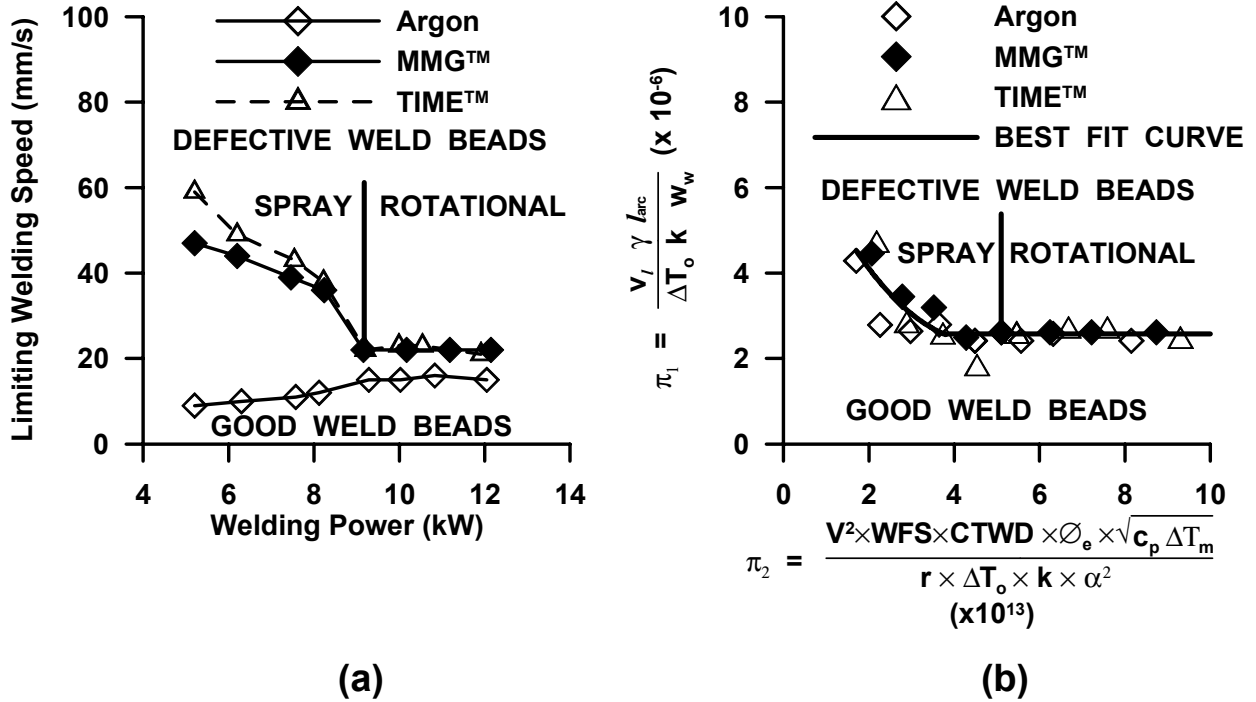


Figure 1: The dimensional GMAW process map of limiting welding speed versus welding power in (a) and the dimensionless GMAW process map of π_1 versus π_2 in (b).

A dimensional analysis of the onset of the high-speed weld defects with respect to various preset GMAW process parameters has shown the following dimensionless variables to be useful:

$$\pi_1 = \frac{v_l \gamma l_{arc}}{\Delta T_o k w_w} \quad (1)$$

$$\pi_2 = \frac{V^2 \times WFS \times CTWD \times \varnothing_e \times \sqrt{c_p \Delta T_m}}{r \times \Delta T_o \times k \times \alpha^2} \quad (2)$$

where π_1 consists of the limiting welding speed, v_l , the influences of the shielding gas; i.e., the surface tension of the molten metal, γ , the ratio between the arc length and the weld width, l_{arc}/w_w , the initial temperature, ΔT_o , and the thermal conductivity of the metal, k . Meanwhile, the dimensionless variable π_2 represents the heat input into the weld pool from the welding arc and the molten filler metal during GMAW. π_2 consists of pre-selected GMAW process parameters such as voltage, V , wire feed speed, WFS, electrode diameter, \varnothing_e , electrical resistivity, r , and contact-tip-to-workpiece distance, CTWD. In π_2 , c_p is the specific heat; ρ is the metal density; α is the thermal diffusivity and ΔT_m is the melting temperature of the metal.

By re-plotting the process map using these new dimensionless parameters, i.e., a plot of π_1 versus π_2 (see Figure 1b), the limiting welding speed data collapses into a single boundary that separates the good and the defective weld bead regions. Initially, this boundary decreases with higher values of dimensionless parameter π_2 . At higher welding powers, i.e., $\pi_2 > 5 \times 10^{13}$, there is a transition from spray to rotational transfer

and π_1 becomes independent of π_2 . High-speed weld defects are predicted to occur for all combinations of π_1 and π_2 that fall above this boundary on the dimensionless plot.

Conclusions

The dimensionless GMAW process map from the present study contains a boundary separating the good from the defective weld bead regions and a transition from spray to rotational transfer modes. Using the dimensionless GMAW process map, the onset of high-speed weld defects can be predicted using the preset process parameters.